

promoting access to White Rose research papers



Universities of Leeds, Sheffield and York
<http://eprints.whiterose.ac.uk/>

This is an author produced version of a paper published in **Journal of Applied Physics**.

White Rose Research Online URL for this paper:
<http://eprints.whiterose.ac.uk/4076/>

Published paper

Schmidt, R. and Brinkman, A.W. (2008) *ac hopping admittance in spinel manganate negative temperature coefficient thermistor electroceramics*, Journal of Applied Physics, Volume 103 (11), 113710.

ac hopping admittance in spinel manganate negative temperature coefficient thermistor electroceramics

Rainer Schmidt^a and Andrew W. Brinkman

Department of Physics, University of Durham, South Road, Durham DH1 3LE, UK

In this work, the ac admittance of a thick film nickel manganate spinel negative temperature coefficient thermistor ceramic system containing a glass phase is investigated. The dominating relaxation process is a grain boundary (GB) effect and has been investigated comprehensively. We present double-logarithmic plots of the specific admittance σ' vs ω and (σ'/σ_{dc}) vs ω , and specific impedance z' vs $-z''/\omega$ and $[(\rho_{dc}/z') - 1]$ vs ω , in order to characterize GB charge transport. Using the complex admittance notation (σ^*), an unusually low Jonscher exponent of frequency ~ 0.007 was obtained and the GB relaxation displayed close to ideal behavior.

PACS numbers: 72.20.-i, 72.20.Ee, 72.80.Ga, 73.40.Cg

Keywords: admittance, Jonscher's law, constant phase element, hopping transport, grain boundary conduction

^a Author to whom correspondence should be addressed. Electronic mail: rainerxschmidt@googlemail.com.
Present address: The University of Sheffield, Engineering Materials, Mappin Street, Sheffield S1 3JD, United Kingdom

Published as:

Rainer Schmidt & Andrew W Brinkman, Journal of Applied Physics, **103** (2008) p113710

I. INTRODUCTION

Strongly correlated electron spinel type manganate oxides exhibit a uniform negative temperature coefficient of resistance (NTCR) between 140 and 520 K without any signs of electronic phase transitions.¹ The direct current (dc) conductivity versus temperature ($\sigma_{dc}-T$) curve in polycrystalline samples has been shown to follow a localized small-polaron hopping model for variable-range hopping (VRH),² typical for transition metal oxides with a strongly localized character of charge carriers. Small-polaron dc hopping conductivity (dc) can be described by the following generalized expression:³

$$\sigma_{dc} = DT^{-\beta} \exp\left(-\frac{T_0}{T}\right)^p \quad (1)$$

where D is the temperature independent contribution to the conductivity, T_0 a characteristic temperature, β describes the pre-exponential temperature dependence, and p the exponential power law dependence. For conventional VRH $0.25 < p = \beta/2 < 0.5$,⁴ for nearest-neighbor polaron hopping (NNH) in the quantum tunneling regime $p = \beta = 1$, and for Boltzmann's thermally activated transport $p = 1$ and $\beta = 0$.⁵ In a previous study, impedance spectroscopy data from thick film nickel manganate were analyzed in the impedance notation. The main impedance contribution was classified as a grain boundary (GB) effect from the specific capacitance, which was in a typical range for GB relaxation processes.⁶ The GB relaxation was dominant in the full frequency range (up to ~ 2 MHz). The thick film impedance was found to be strongly dominated by the GB resistance, which showed approximately identical $\sigma_{dc}-T$ behavior compared to the dc curve of NiMn_2O_4 pellets. This implies that bulk and electrode interface resistance, and contributions from the thick film glass phase are insignificant.

Here, the complex admittance notation is used, which can reveal a great deal of additional information, to further characterize the alternating current (ac) hopping transport. The extraction of critical frequency exponents was achieved by determining the slope of double-logarithmic plots of various expressions versus frequency ω . Such plots require data representation in the admittance notation (the method is then often termed admittance spectroscopy). Critical exponents are commonly extracted only for intrinsic bulk contributions at the high frequency end, but not for GB relaxation processes. GB and bulk relaxation processes often show strong overlap in admittance and impedance spectra, which hinder the detailed analysis of intermediate frequency GB relaxation. Here, the absence of a perceptible contribution from a bulk relaxation process allowed studying the pure GB conduction in detail.

II. COMPLEX ADMITTANCE AND IMPEDANCE

The complex specific impedance $z^* = (z_{-} + iz_{+})$ or specific admittance $\sigma^* = (\sigma' - i \sigma'')$ of electrode interface, GB, and bulk relaxation phenomena in polycrystalline materials are commonly described by a parallel resistor–capacitor circuit (RC element).⁷ In the complex admittance notation [$\sigma^* = (z^*)^{-1}$] parallel circuit elements are additive, leading to a simple expression for the complex admittance σ_{RC}^* of a single ideal RC element as follows:

$$\sigma_{RC}^*(\omega, T) = \sigma_{dc}(T) + i\omega c' \quad (2)$$

where σ_{dc} is the dc conductivity of the resistor and c' the real part of the specific capacitance ($c' = \epsilon_0 c'$), and ϵ_0 and ϵ_r are permittivity of vacuum and relative permittivity of the respective relaxation in the sample. In reality, few systems behave in a perfect Debye manner as represented by ideal resistors and capacitors. In order to account for non-Debye response, ideal capacitors are commonly replaced by constant-phase elements (CPEs).⁸ CPEs exhibit a frequency independent constant-phase angle with respect to the response from an ideal capacitor. In the complex admittance notation, a CPE replacing an ideal capacitor is given by

$$\sigma_{CPE}^* = (i\omega)^n c_m' \quad (3)$$

where n is an empirical parameter close to 1: $n \leq 1$ and c_m' is the real specific capacitance in modified units of $F s^{n-1}$. This leads to the following real part admittance σ' for the widely used R -CPE circuit of parallel resistor and nonideal CPE capacitor, using the relationship $(i)^n = \cos(n\pi/2) + i \sin(n\pi/2)$:

$$\sigma' = \sigma_{dc} + c_m' \omega^n \left(\cos \frac{n\pi}{2} \right) \quad (4)$$

which can be expressed in the following simplified form:

$$\frac{\sigma'}{\sigma_{dc}} = 1 + A \omega^n \quad (5)$$

where A is a material and sample specific expression containing all frequency independent parameters. Equation (5) corresponds to Jonscher's universal response law,⁹ and applies to almost all localized electron hopping systems known.

Whereas Eq. (5) scales the high frequency dependence of σ' in hopping systems, several further attempts can be found in literature to scale the temperature dependence as well. For a wide range of materials, data sets of σ' vs ω taken from one sample at various temperatures can be plotted in one single master curve:^{10,11}

$$\frac{\sigma'}{\sigma_{dc}} = 1 + \left(\frac{C \alpha e^2 \omega}{k_B T \sigma_{dc}} \right)^M \quad (6)$$

where C is a constant, α the reciprocal electron localization length, e elementary charge, k_B Boltzmann's constant, and M an empirical factor. Expression (6) has been suggested for localized electron ac hopping in conventional semiconductors in the low temperature impurity conduction regime, with R values of $R = 0.725$ (Ref. 10) and $R = 0.8$.¹² Applying the relationship between Jonscher's law and CPE exponent (Eqs. (4) and (5)), such ω dependence may be associated with an R -CPE equivalent circuit with $M = n$.

Universal expressions such as Jonscher's law (5) and the universal scaling law (6) are preferably expressed in the admittance notation; other formalisms yield more complicated expressions. For example, the simplest universal expression for the real part of impedance z' of an R -CPE circuit may be expressed in the form of

$$\frac{\rho_{dc}}{z'} = \frac{1 + 2A\omega^n + B\omega^{2n}}{1 + A\omega^n} \quad (7)$$

where A and B are frequency independent material and sample specific constants. In the high frequency limit ($\omega \rightarrow \infty$), Eq. (7) shows an effective ω^n dependence ($n < 1$) and an ω^2 dependence for an ideal RC element ($n = 1, A = 0, B = [c \rho_{dc}]^2 = \tau^2$), where τ is the relaxation time of the respective RC element and ρ_{dc} the resistivity of the resistor R .

III. EXPERIMENTAL

The production of thick film NTCR spinel manganate samples ($\sim 25 \mu\text{m}$) containing a glass phase has been described elsewhere.¹³ It was shown previously that the macroscopic impedance at $T \geq 120^\circ\text{C}$ can be fitted precisely with an equivalent circuit containing a series of one R -CPE and one RC element representing interface and GB contributions.⁶ A detailed description of the experimental setup for ac impedance spectroscopy between 60 – 220°C using a HP 4192A LF impedance analyzer at frequencies of 5 Hz – 6 MHz can be found elsewhere.¹⁴ The data shown here were all cut at 2 MHz , in order to not display data dominated by noise contributions. This has been shown to be appropriate in many instances previously.^{7,15}

IV. RESULTS AND DISCUSSION

Impedance (admittance) spectroscopy data obtained from thick film nickel manganate are plotted in Fig. 1 between 60 – 220°C on double-logarithmic z' vs $-z''/\omega$ axes. This data representation was suggested by Abrantes *et al.*¹⁶ The inset figure shows conventional complex plane impedance plots of $-z''$ vs z' . Plots of z' vs $-z''/\omega$ clearly display two distinctively different regimes. The intermediate/high frequency contribution arises from the dominating high resistance GB contribution. The low frequency contribution can be identified as an electrode sample interface effect, which cannot be resolved from the $-z''$ - z' semicircle arcs due to relatively low contact resistances.

Good linearity of the main GB contribution in z' vs $-z''/\omega$ (Fig. 1) indicates the presence of an approximately ideal capacitance. For a nonideal R -CPE circuit, the curves would show convex bending. The 60 – 100°C curves show deviation from linearity at high frequency, which indicates high frequency noise. For a typical bulk contribution, an additional abrupt drop in the curve at high frequencies would be expected, in contrast to the observed gradual upturn. The analysis of double-logarithmic plots of σ' versus frequency (Fig. 2) confirmed quasi-ideal behavior: σ' is approximately independent of ω as expected for an ideal relaxation (Eq. (2)), and $\sigma' = \sigma_{dc}$. In order to investigate the ω dependence of σ' in more detail, the exponent n (Eq. (5)) was determined by plotting $\log(\sigma'/\sigma_{dc})$ vs $\log(\omega)$. Figure 3 displays $\log(\sigma'/\sigma_{dc})$ approximately independent of ω at low frequency, in the intermediate range a slope of $q \sim 0.007$ indicates an exponential $\omega^{0.007 \pm 0.001}$ dependence, and at high ω a larger exponent of $n \sim 1$ shows. The intermediate behavior dominated by the GB contribution was interpreted as a manifestation of a quasi-ideal relaxation process. The value of $q = 0.007$ is one of the lowest values reported in hopping systems known to the authors, and is close to frequency independent behaviour of an ideal RC element. At high frequency, an upturn of the curve indicates a rapid increase of the ω exponent, which could potentially be a manifestation of a high frequency bulk relaxations process. This upturn occurs at relatively high frequency though and noise contributions may be the likelier explanation. In the inset of Fig. 3, data are plotted as $\log(\sigma'/\sigma_{dc})$ vs $\log(\omega T^4 / \sigma_{dc})$ in order to establish a master curve where all data points accumulate. An empirical T dependence of $T^{4 \pm 1}$ had to be assumed, which leads to the following purely empirical scaling law:

$$\frac{\sigma'}{\sigma_{dc}} = 1 + \left(\frac{T^4 \omega}{C^{\sim} \sigma_{dc}} \right)^{0.007} \quad (8)$$

where C^{\sim} contains all frequency and temperature independent parameters. In order to extract the ω exponents in the impedance notation, data were plotted as $\log([\rho_{dc}/z'] - 1)$ vs $\log(\omega)$ (Fig. 4). In the inset of Fig. 4, it can be seen that all data points accumulate on a master curve scaled with ρ_{dc} , if no temperature dependence is used at all. Obviously, scaling with ρ_{dc} and σ_{dc} leads to very different temperature dependencies, which demonstrate the completely empirical and somewhat random nature of master curve scaling of the ac hopping temperature dependence. In fact, the scaling presented in the inset of Fig. 3 is not ideal. A crossover from ω^1 to ω^2 behavior is indicated in Fig.4, which corresponds to nonideal and quasi-ideal relaxations, respectively [Eq. (7)]. The low frequency electrode interface contribution may therefore be attributed to a nonideal capacitance. This can be explained by the expected reduced dimensionality of the interface.¹⁷ The quasi-ideal behavior of the GB relaxation displayed in the impedance notation confirms the results obtained previously from the admittance notation.

V. CONCLUSIONS

In conclusion, it has been shown that ac hopping conductivity in ceramic spinel manganates results in an unusually low exponential ω dependence of the admittance σ'/σ_{dc} of $q = 0.007 \pm 0.001$. Quasi-ideality of the relaxation process was identified by the lack of a higher ω exponent and in a ω^2 dependence of the normalized impedance ρ_{dc}/z' . At low frequency, a dependence of $\rho_{dc}/z' \sim \omega^1$ indicated the presence of a nonideal electrode interface relaxation. For data fitting, it may be most reasonable to employ an equivalent circuit of one R -CPE (interface) and one RC (GB) element in series, which has been indeed shown previously to lead to reasonable fits.⁶ Double-logarithmic $\log(\sigma'/\sigma_{dc})$ vs $\log(\omega)$ and $\log(\{\rho_{dc}/z'\}-1)$ vs $\log(\omega)$ type plots were shown to be powerful tools to determine critical ω exponents. Empirical universal scaling laws allowed plotting all frequency and temperature dependent data in the admittance and impedance notation in purely empirical master curves. Using the z' vs $-z''/\omega$ plots of Abrantes *et al.*, the low frequency electrode interface contribution could be deconvoluted. No clear indications for a high frequency bulk relaxation were detected.

ACKNOWLEDGMENTS

The authors wish to thank Michael Petty for allowing use of the ac impedance spectroscopy facility. Thanks to Finlay Morrison and Ian Terry for useful discussions concerning impedance spectroscopy data analysis. Thanks to Andreas Roosen and Alfons Stiegelschmitt for the guidance provided in developing thick film samples.

REFERENCES

- ¹J. A. Becker, C. B. Green, and G. L. Pearson, *Bell Syst. Tech. J.* **26**, 170 (1947).
- ²R. Schmidt, A. Basu, and A. W. Brinkman, *Phys. Rev. B* **72**, 115101 (2005).
- ³R. Schmidt, A. Basu, A. W. Brinkman, Z. Klusek, and P. K. Datta, *Appl. Phys. Lett.* **86**, 073501 (2005).
- ⁴B. I. Shklovskii and A. L. Efros, *Electronic Properties of Doped Semiconductors* (Springer-Verlag, Berlin, 1984).
- ⁵U. Weiss, *Quantum Dissipative Systems* (World Scientific, Singapore, 1999).
- ⁶R. Schmidt and A. W. Brinkman, *Adv. Funct. Mater.* **17**, 3170 (2007).
- ⁷J. T. S. Irvine, D. C. Sinclair, and A. R. West, *Adv. Mater. (Weinheim, Ger.)* **2**, 132 (1990).
- ⁸*Impedance Spectroscopy*, edited by J. R. Macdonald (Wiley, New York, 1987).
- ⁹A. K. Jonscher, *J. Non-Cryst. Solids* **8–10**, 293 (1972).
- ¹⁰S. Summerfield, *Philos. Mag. B* **52**, 9 (1985).
- ¹¹S. Abboudy, P. Fozooni, R. Mansfield, and M. J. Lea, *Philos. Mag. Lett.* **57**, 277 (1988).
- ¹²M. Pollak and T. H. Geballe, *Phys. Rev.* **122**, 1742 (1961).
- ¹³R. Schmidt, A. Basu, A. W. Brinkman, Z. Klusek, W. Kozłowski, P. K. Datta, A. Stiegelschmitt, and A. Roosen, *Appl. Surf. Sci.* **252**, 8760 (2006).
- ¹⁴R. Schmidt and A. W. Brinkman, *J. Eur. Ceram. Soc.* **25**, 3027 (2005).
- ¹⁵R. Schmidt, in *Ceramic Materials Research Trends*, edited by P. B. Lin (Nova Science, Hauppauge, 2007).
- ¹⁶J. C. C. Abrantes, J. A. Labrincha, and J. R. Frade, *Mater. Res. Bull.* **35**, 727 (2000).
- ¹⁷S. H. Liu, *Phys. Rev. Lett.* **55**, 529 (1985).

FIGURE CAPTIONS

FIG. 1. (Color online) z' vs $-z''/\omega$ plots of Abrantes *et al.* on double-logarithmic axes (\square = data, \blacksquare = model) at $T = 60\text{--}220^\circ\text{C}$; irregular behavior at high ω for $T = 60\text{--}100^\circ\text{C}$ is displayed; at $T \geq 120^\circ\text{C}$ regular fits were obtained using a series of a R -CPE (interface) and RC (GB) element. Inset: conventional $-z''$ vs z' plots.

FIG. 2. (Color online) σ' vs ω on double-logarithmic axes for $T = 120\text{--}220^\circ\text{C}$ (\square = data, \blacksquare = model); good linearity indicates an approximately ideal capacitor; curves equidistant on the $\log(\sigma')$ axis at various T confirm the exponential T dependence of GB hopping conductivity.

FIG. 3. (Color online) $\log(\sigma'/\sigma_{\text{dc}})$ vs ω , Inset: $\log(\sigma'/\sigma_{\text{dc}})$ vs $(\omega T^4)/\sigma_{\text{dc}}$ using logarithmic x -axes.

FIG. 4. (Color online) $(\rho_{\text{dc}}/z') - 1$ vs ω , Inset: ρ_{dc}/z' vs $\omega\rho_{\text{dc}}$ using double-logarithmic axes.

Fig 1

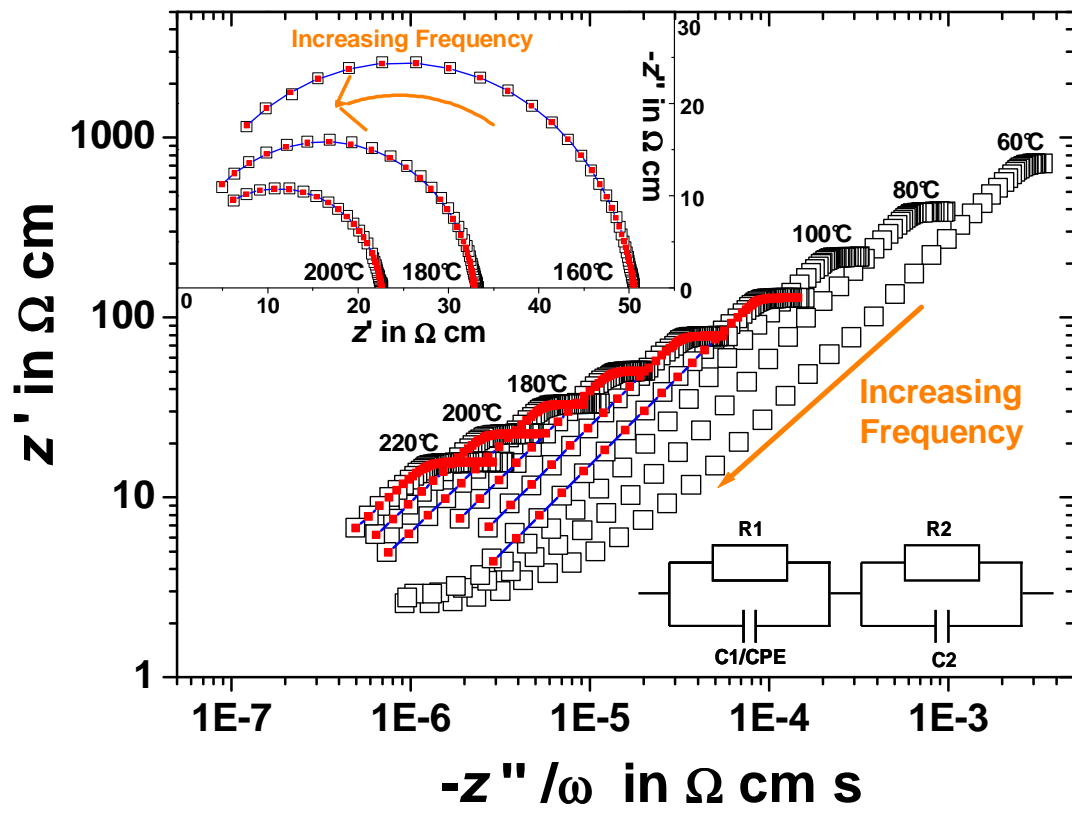


Fig 2

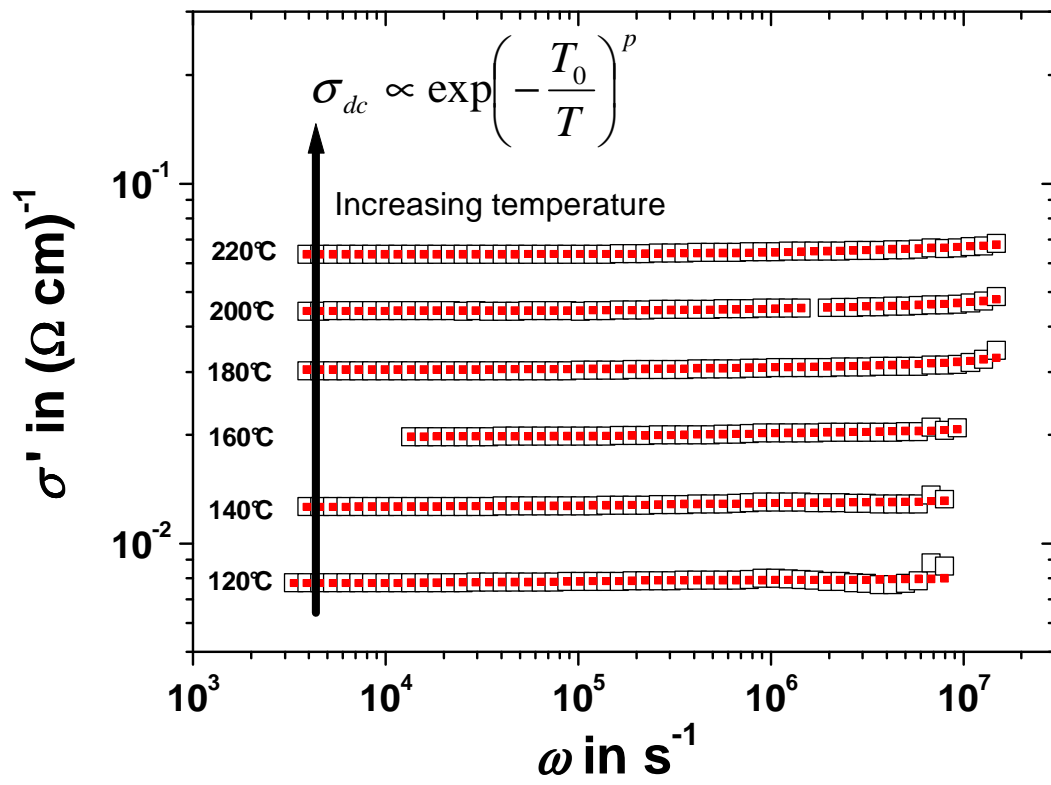


Fig 3

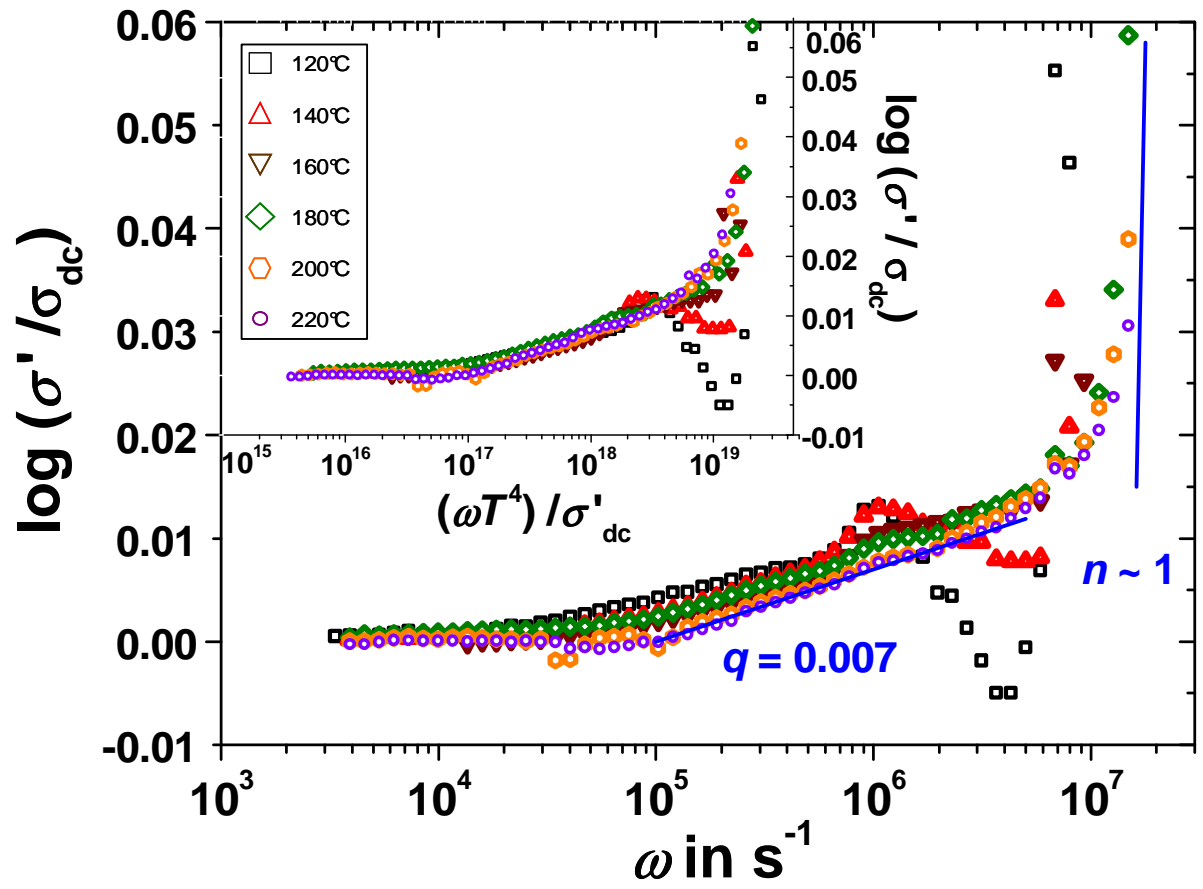


Fig 4

